SANDIA REPORT

SAND87—2119 • UC—212
Unlimited Release
Printed December 1989

Final Report of Lithium Ambient-Temperature Battery Reliability

Calvin D. Jaeger, Edward V. Thomas

Prepared by
Sandia National Laboratories
Albuquerque, New Mexico 87185 and Livermore, California 94550
for the United States Department of Energy
under Contract DE-AC04-76DP00789

Issued by Sandia National Laboratories, operated for the United States Department of Energy by Sandia Corporation.

Printed in the United States of America. This report has been reproduced directly from the best available copy.

Available to DOE and DOE contractors from
Office of Scientific and Technical Information
PO Box 62
Oak Ridge, TN 37831

Prices available from (615) 576-8401, FTS 626-8401

Available to the public from
National Technical Information Service
US Department of Commerce
5285 Port Royal Rd
Springfield, VA 22161

NTIS price codes
Printed copy: A02
Microfiche copy: A01

SAND87–2119
Unlimited Release
Printed December 1989

Distribution
Category UC–212

Final Report of Lithium Ambient-Temperature Battery Reliability

Calvin D. Jaeger
Exploratory Batteries Division
Edward V. Thomas
Statistics, Computing, and Human Factors Division
Sandia National Laboratories
Albuquerque, NM 87185

Abstract

A program to develop nondestructive testing techniques to enable prediction of the reliability of primary lithium cells has been underway since FY 1981. Various candidate techniques, such as microcalorimetry and complex impedance analysis were considered and tried. Statistical analysis of available data from this program indicates that several measurements derived from complex impedance analysis directly relate to the capacity condition of the cell. These measurements could form the basis for predicting cell performance and therefore cell reliability for a particular application.

Contents

Figures

Tables

Final Report of Lithium Ambient-Temperature Battery Reliability

Introduction

The objective of this program was to develop a nondestructive testing methodology to predict the performance of primary lithium cells for long-life applications. If the performance predictions are accurate, then the nondestructive techniques can be used to effect a screen in order to improve battery reliability. The nondestructive techniques that were used in this study were open-circuit voltage measurements, complex impedance analysis, and microcalorimetry. The tests supporting this program used three different groups of Li/SO_2 D-cells—PM (cells of an old design without improved glass-to metal seals), NE (cells of similar design to PM cells but with TA-23 glass-to-metal seals), and SM (Sandia modified cells). Further information on these cells and the results for the PM and NE cells can be found in the references in Appendix A.

The references in Appendix A also provide further information about this program and an explanation of some of the data formats and terminology used in this report. The first three reports covered the periods of May 1981 through April 1982, May 1982 through April 1983, and May 1983 through April 1985. This new report covers the work done by Sandia National Laboratories from May 1985 to the end of the program. The program results and discussions, as well as the subsequent data analysis, will concern the SM cells. Earlier reports presented the results for the PM and NE groups.

Program Activities

May 1981 - April 1982

Laboratory space was obtained and equipped. The test matrix was defined. Cells for the test program were selected and purchased. The evaluation and development of electrochemical and analytical techniques were begun. Software was developed for the complex impedance measurements and a simple curve-fit program was written. Experimental work was begun. Complex impedance measurements were performed using an HP4192 Impedance Analyzer and an HP9826 computer. Microcalorimetry measurements were made using a Tronac 351-RA Battery Calorimeter. The microcalorimetry results were recorded on a strip recorder.

May 1982 - April 1983

The battery reliability laboratory was completed. Low-frequency impedance capability was developed using an HP3325 Function Analyzer and HP9242 Multiprogrammer. A WICAT 150S Computer and a Hart microcalorimeter were obtained and further data acquisition and analysis were performed using the computer. The baseline cells for the first two groups (PM and NE) were completed. All of the cells for the test matrix were received. The test matrix was begun for the PM and NE cells.

May 1983 - April 1985

A data management system was developed for handling the program data. Most data was transferred to the HP3000. The data acquisition and analysis system for the microcalorimeters was refined. A complex least-squares curve-fit algorithm was developed to fit the complex impedance data. Measurements for the PM cells were completed. Some of the PM cells failed during storage. A preliminary statistical analysis was performed on the available data. Problems with the WICAT 150 computer and microcalorimeters continued to hamper accomplishment of the test matrix.

May 1985—June 1987

All cell measurements were completed. A comprehensive analysis was performed on the experimental data for the SM cells with the primary objective being to find parameters derived from the various nondestructive analyses that relate to performance (capacity). A regression tree analysis was found to be the most informative type of analysis.

Results and Discussion

Test Matrix

To support this program, a test matrix was designed. The test matrix, consisting of 140 fresh, spirally-wound Sandia modified D-cells from a single lot, stored under various conditions and discharged at various rates, is outlined in Table 1. Each group of cells (PM, NE, and SM) had an identical test matrix. Initially all cells had complex impedance and open-circuit voltage measurements performed to establish a frame of reference for each cell. On the cells to be discharged at 57 and 0.8 Ω, microcalorimetry measurements were also performed. All cells were stored at a mildly accelerated-aging temperature of 40°C, half at open circuit (OC) and half under a light-load of 7500 Ω (LL), except for 20 cells which were discharged immediately (baseline cells, BL). Prior to discharge, nondestructive tests were performed on all cells. The cells were then discharged at one of the five rates specified by the test matrix.

Table 2 shows the cell assignments within the test matrix for the SM group. The SM cells used TA-23, the Sandia-developed corrosion-resistant glass. Some SM cells were filled a few days after the others. Although the cells are of the same design, the data from the cell measurements for these last ten cells differ from those of the other SM cells.

Table 1. Test matrix for battery reliability program

LOAD,Ω FINAL DISCHARGE	0 yr	0.5 yr		1.0 yr		1.5 yr	
		OC	LL	OC	LL	OC	LL
57		X	X	X	X	X	X
11							
5.5							
3							
0.8		X	X	X	X	X	X

NOTE: 4 CELLS TESTED AT EACH CONDITION. MICROCALORIMETRIC MEASUREMENTS ARE INDICATED BY X

OC = OPEN CIRCUIT
LL = LIGHT LOAD

Table 2. Test matrix for SM Cells – 40°C storage temperature

	0.5 YR		1.0 YR		1.5 YR		0 YR
	OC	LL	OC	LL	OC	LL	
*R_1 57Ω	93 94 95 96	101 102 103 104	125 126 127 128	133 134 135 136	109 110 111 112	117 118 119 120	1 2 3 4
R_2 11Ω	21 22 23 24	41 42 43 44	33 34 35 36	69 70 71 72	57 58 59 60	81 82 83 84	5 6 7 8
R_3 5.5Ω	29 30 31 32	45 46 47 48	37 38 39 40	73 74 75 76	61 62 63 64	85 86 87 88	13 14 15 16
R_4 3Ω	25 26 27 28	49 50 51 52	53 54 55 56	77 78 79 80	65 66 67 68	89 90 91 92	17 18 19 20
*R_5 0.8Ω	97 98 99 100	105 106 107 108	129 130 131 132	137 138 139 140	113 114 115 116	121 122 123 124	9 10 11 12

* CELLS (EXCEPT 0 YEAR) DESIGNATED FOR MICROCALORIMETRY.

NOTE: ALL SM CELLS ON STORAGE
ACTUAL CELL NUMBERS SHOWN INSIDE MATRIX.

Capacity Measurements

Figure 1 displays the observed relationships between median remaining capacity (each data point represents the median value for four cells) and discharge rate for the range of storage conditions for the SM group.

The load applied during the final discharge clearly affected the remaining capacity. From Figure 1, it is clear that the discharge rate effect is strongest for the LL cells. It is also clear that there is a loss of capacity in the LL cells over and above that due to the capacity removed during storage, approximately 0.28 Ah per month.

Figure 2 shows how the total capacity (including that removed during storage) changes with respect to storage time for low-rate (LR≈0.05A) and high-rate (HR ≈ 1.0A) final discharges. For OC cells, the LR discharge suffered a 0.45 Ah/year capacity loss and the HR discharge had a 0.95 Ah/year capacity loss. For the LL cells, the LR discharge suffered a 2.95 Ah/year capacity loss and the HR discharge suffered a 5.10 Ah/year capacity loss. Only part of the actual capacity loss can be explained by a "true" loss in capacity (capacity, removed during storage). Part of the capacity loss, even at low rates, is due to a loss of rate capability.

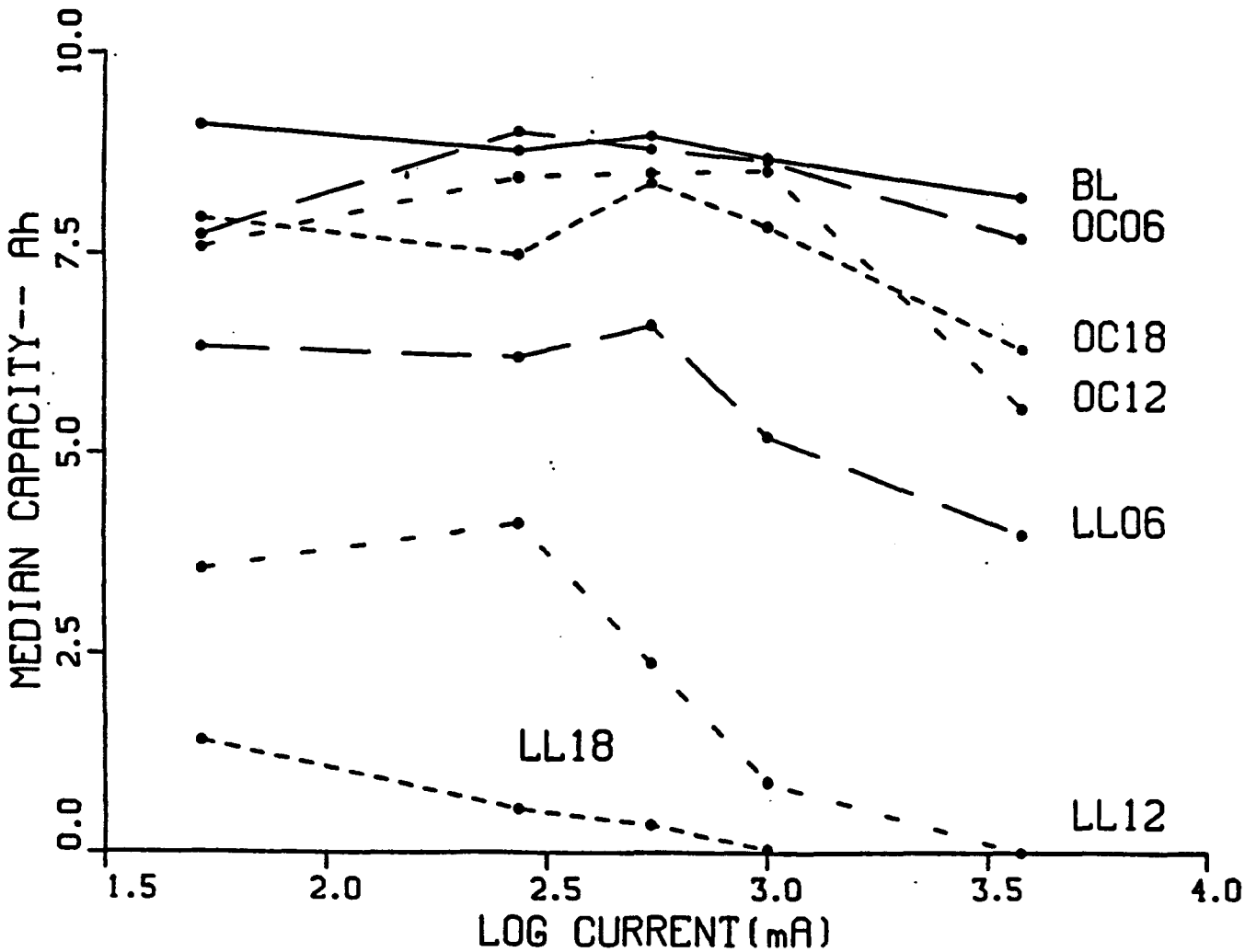

Figure 1. Selim-Bro plot of remaining capacity versus discharge current. Performance of SM cells after storage.

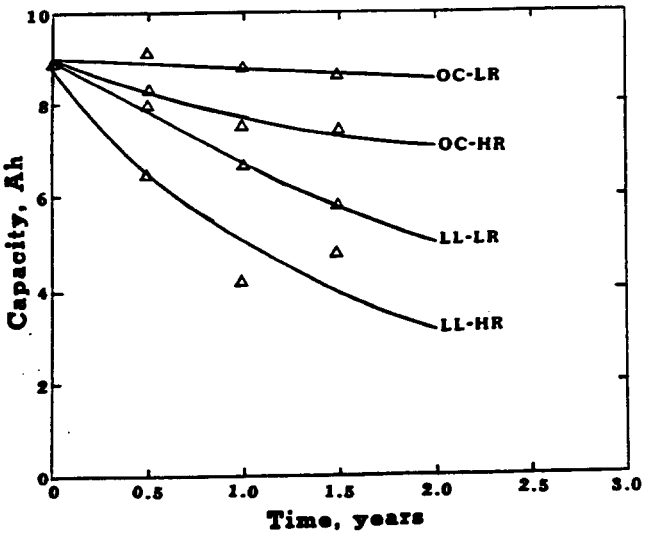

Figure 2. Total capacity versus storage time at 40°C. HR – high rate (1.0A); LR – low rate (0.05A).

Cell Voltage

Cell voltage measurement is the easiest of the nondestructive techniques that can be applied to a cell. In our study, we identified a number of anomalous factors that affect the cell voltage, e.g., electrolyte decomposition during storage at elevated temperatures, and discharge through an internal load (e.g., short across the glass-to-metal seal). Although the influence of some of these factors was readily apparent, open-circuit voltage did not prove to be a reliable indicator of the residual capacity. Generally, the cell voltage for the OC cells continually increased over the 18-month period. In the case of the LL cells, the cell voltage reached some maximum between 12 and 18 months. This maximum is a cell's voltage while under discharge and may be attributed to the influence of the bulk electrolyte conductivity effect. Figure 3 shows, using a "box and whisker" plot, how open-circuit voltage changes with respect to the various storage regimes. The top and bottom of the "whiskers" represent the range of values for this data set. Note that each box and whisker diagram summarizes the distribution of OCVs for 20 cells. The top of the box represents the 75th percentile and the bottom of the box represents the 25th percentile. The line inside the box represents the median value (50th percentile) for the data set.

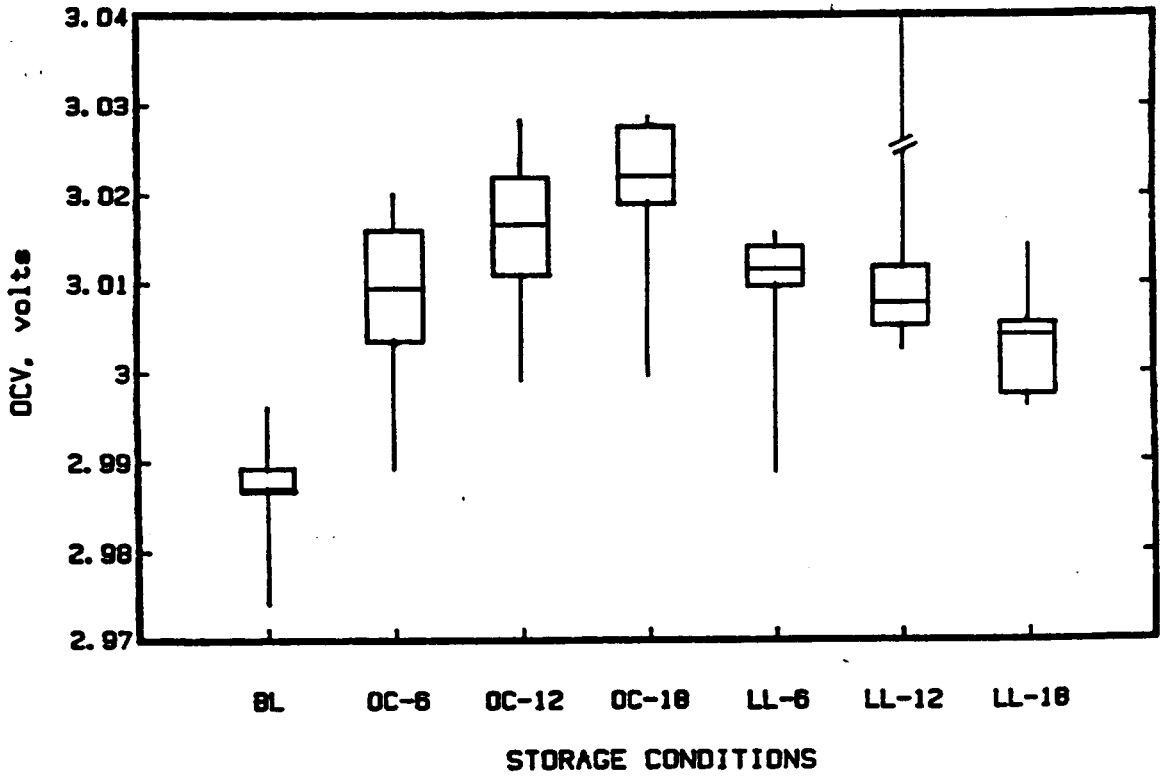

Figure 3. Distribution of OCV values versus storage conditions. BL – baseline; OC – open-circuit storage; LL – light-load storage; storage period: 6, 12, and 18 months.

Microcalorimetry

Microcalorimetry is a very sensitive technique that enables one to measure heat flux in the microwatt range. Although microcalorimetery has been used quite satisfactorily with certain heart pacemaker batteries, we were unable to relate the measured heat output to the residual cell capacity. Generally, the magnitude of the heat flux was too small to account for significant capacity loss. Most cells stabilized to about 20 μW after highly random initial heat values (Table 3). Early-life microcalorimetry measurements are probably of no diagnostic value because of this great variability. Microcalorimetry may be useful as a system characteristic after some storage period. A heat flux of 20 μW for a Li/SO_2 D-cell is roughly equivalent to a corrosion current of 8 μA. This translates to about only 0.07 Ah/year capacity loss.

Complex Impedance Analysis

The complex impedance spectrum for a Li/SO_2 D-cell consists of contributions from three different sources. The vector sum of these three elements over the given frequency range yields the total cell impedance. The three elements are the ohmic component, the lithium anode impedance, and the porous carbon cathode collector impedance. Figure 4 shows the relative contributions of each of these components. In general, the large semicircular component(s) of the spectrum can be attributed to the passive film on the lithium anode, and the linear region at lower frequencies can be ascribed to the contribution from the porous carbon cathode collector.

Figure 5 shows another typical complex impedance spectrum for the cells being studied in this program, with ten impedance parameters identified that were used to characterize the spectrum. Estimates of these parameters were obtained using a nonlinear least-squares regression program. As previously shown in an earlier report, this curve-fitting algorithm provides an excellent fit of the experimental data.

The ohmic component is represented by the high-frequency intercept, R1. This parameter is related to the bulk electrolyte resistance plus other "bulk" effects such as solid resistances and uncompensated lead resistances. The impedance of the leads, which can contain a considerable inductive component, is compensated for during the cell measurements. In some instances at the very high frequencies, a small inductive component is observed, which may possibly be due to the geometry of the cell's electrodes (e.g., a spirally wound cell).

Table 3. Mean heat fluxes and standard deviations for SM cells (μW)

	Before Storage		After Storage	
Cell	Mean	Std. Div.	Mean	Std. Div.
93	32.3	0.80	15.0	0.72
94	32.2	0.47	17.3	1.8
95	0.575	1.8	23.5	1.6
96	33.9	1.5	18.5	4.2
97	0	0	19.3	1.5
98	2.13	2.0	20.6	1.7
99	41.6	0.71	19.8	2.4
100	29.2	0.74	15.4	2.3
101	10.5	0.37	24.1	1.9
102	18.8	0.91	18.0	1.2
103	12.4	0.71	25.2	2.0
104	59.0	1.1	20.8	1.7
105	13.3	0.34	14.2	0.74
106	11.2	1.1	18.2	1.5
107	11.1	0.85	19.7	1.8
108	10.6	0.47	14.4	0.94
109	31.9	0.34	28	
110	48.4	0.69	23	
111	6.81	1.3	22	
112	23.1	0.53	34	
113	46.6	0.97	24	
114	8.70	0.55	16	
115	29.2	0.42	20	
116	25.7	0.61	20	
117	5.57	0.32	35	
118	56.5	3.2	33	
119	24.0	0.46	35	
120	16.0	0.36	9500	
121	28.4	1.0	39	
122	151.5	0.65	675	
123	11.0	0.46	41	
124	28.5	0.19	44	
125	9.75	0.66	27	
126	9.29	0.48	13	
127	12.8	1.6	16	
128	8.00	0.66	16	
129	34.4	0.48	16	
130	45.6	3.2	14	
131	86.6	0.42	33	
132	78.4	0.68	32	
133	97.4	0.57	30	
134	90.0	0.58	25	
135	71.9	0.44	26	
136	123	0.38	19	
137	67.5	0.31	29	
138	91.9	0.31	25	
139	95.7	0.51	28	
140	69.4	0.92	25	

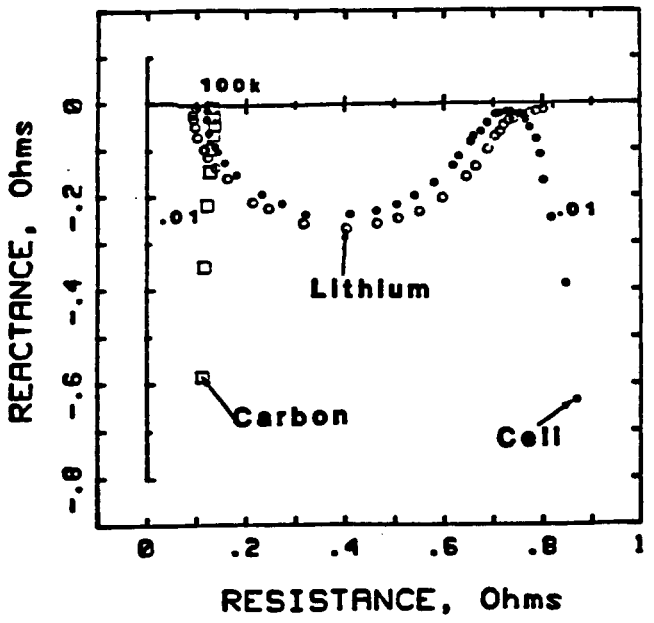

Figure 4. Contribution of cell components to impedance in a Li/SO_2 D-cell

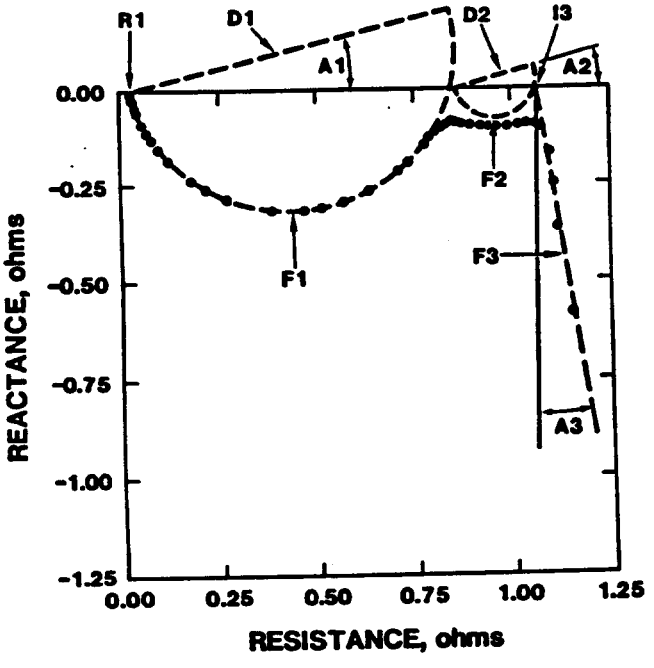

Figure 5. Complex impedance spectrum parameters for Li/SO_2 D-cell

Under open-circuit storage conditions, the ohmic component changes only as a result of electrolyte decomposition, resulting in a decrease of SO_2 concentration and possibly the buildup of a solid reaction product within the porous carbon cathode. As will be shown later, no significant change in R1 was noted for the open-circuit storage cells. As cells are discharged, two things occur that may affect the magnitude of R1: (1) the concentration of SO_2 decreases, affecting the bulk electrolyte conductivity (Figure 6), and (2) approximately 17% of the SO_2 is removed during a six-month period for the light-load cells. Figure 7 shows how R1 changes with respect to storage condition.

The OC cells show no change in R1, whereas R1 increases almost linearly for the LL cells. From Figure 6, it is apparent that the increase in R1 cannot be attributed to changes in the electrolyte conductivity because conductivity first increases and then decreased during discharge. In addition, a solid reduction product, lithium dithionite ($Li_2S_2O_4$), builds up within the porous carbon cathode collector. We attribute the changes in R1 for the light-load cells to this factor.

The lithium anode is represented by one or two semicircular elements considered to be in series; each semicircular element consists of three variables. The variables for the first semicircle are the diameter, D1; the skew angle, A1; and the frequency at the maximum reactance, F1. The second semicircle has similar variables—D2, A2, and F2. Although we believe this second semicircle is related to the lithium passive film, we have not assigned any specific physical significance to it. The values for the second semicircle were quite inconsistent and were not found to be related to cell performance.

For the first semicircle, the diameter and frequency of the semicircular components can be related to the properties of the lithium passive film. In earlier laboratory experiments, the activation energies were estimated from the semicircular component of the spectra of both Li/SO_2 D-cells and Li electrodes (in similar electrolyte, over a temperature range from −30°C to 70°C). The estimated activation energies were the same for both experiments (0.63 eV). Likewise, the capacitance derived from the semicircular component is characteristic of a dielectric film. The values of D1 and F1 can be used to estimate the film's capacitance and an apparent film thickness.

Figure 8 shows how D1 changes with respect to storage condition. D1 increases for both the OC and LL cells. For the OC cells, D1 increases about 2.7 Ω/year. For the LL cells, D1 increases about 2.8 Ω/year. The increase in D1, being nearly the same, whether cells are at OC or LL, is suggestive of a continuous increase in the cell impedance, regardless of any external load being placed on the cell. In another program that used Li/SO_2 D-cells, the value for D1 was found to increase with increasing temperature (T) according to the following expression:

$$\text{Log}(D1) = a + bT + \epsilon,$$

where a and b are constants and ϵ is a random error.

The physical significance of the skew angle, A1, is less clear. In almost all lithium ambient-temperature batteries, the semicircular component ascribed to the lithium passive film is not centered on the resistance axis. Several explanations have been offered to explain this skewing; they include a distribution of relaxation constants, nonuniform surface coverage, and electrode roughness. As will be discussed later, the skew angle does change as capacity is removed from the cells. Besides the physical causes for this occurrence there is also another reason for this trend in our study, arising from the fact that the fitting-function used to curve-fit the data involves a semicircle. To adequately fit some of the data, the semicircle must be significantly displaced off the resistance axis. The parameter A1 is particularly sensitive to the qualitative shape of the semicircular component. Figure 9 shows the complex impedance spectrum for a cell stored at open-circuit conditions and one stored under light-load conditions, after 18 months' storage at 40°C. In the high-frequency region, cells that have been discharged appear to have a linear region. To fit this region using a semicircle, the semicircle must be displaced to greater degree off the resistive axis. This results in larger A1 values for light-load cells. Figure 10 shows how A1 changes with respect to storage condition. A reasonable physical explanation of what is causing this flattening of the semicircle at the high-frequency region has not been developed at this time. This phenomenon occurs for all discharged cells and may be due to changes in the physical and electronic properties of the lithium anode as a result of being discharged (e.g., increased anode roughness, dielectric film).

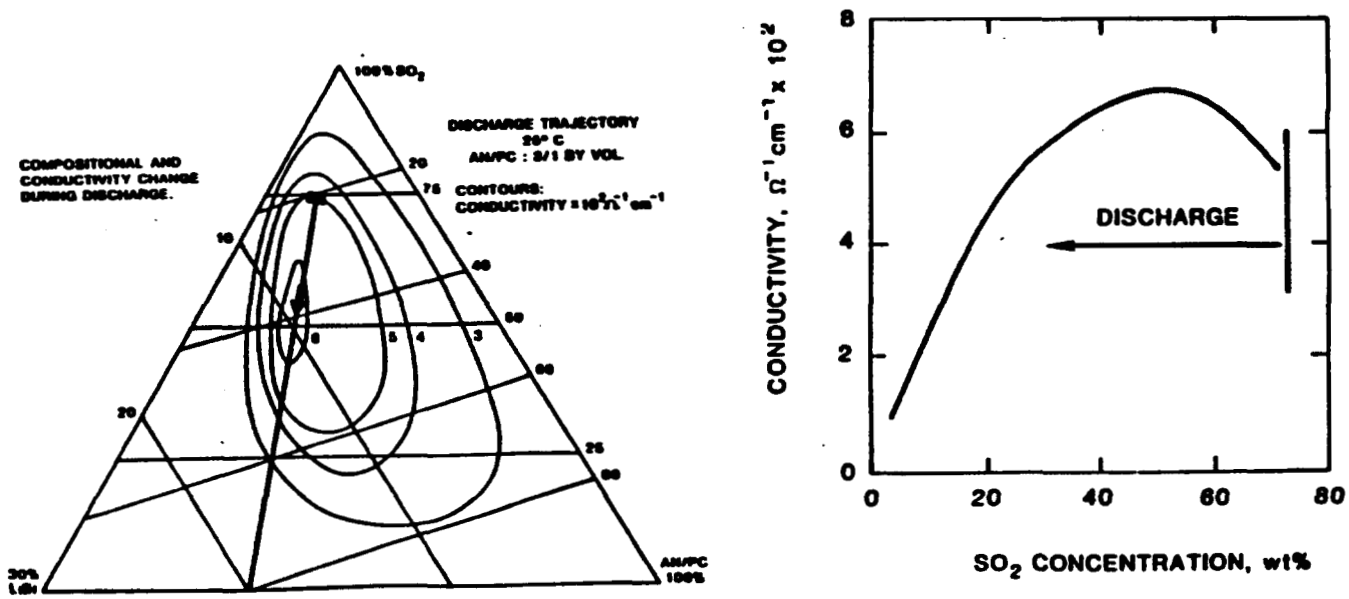

Figure 6. Changes of electrolyte conductivity as a function of SO_2. The figure on the left is for a mixed acetonitrile/PC electrolyte.

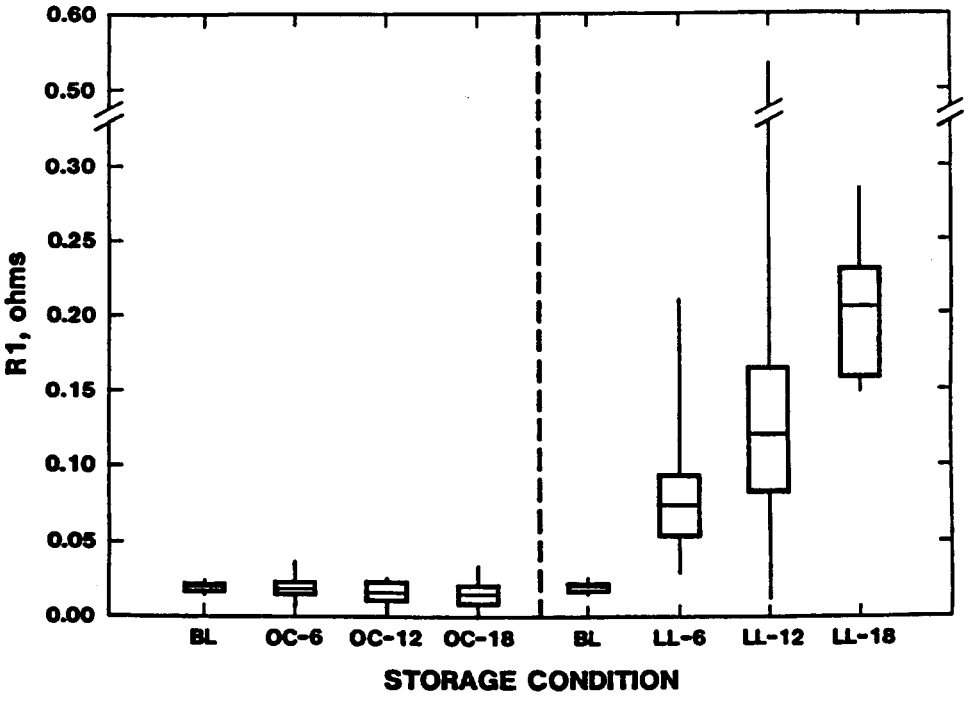

Figure 7. Distribution of R1 values versus storage conditions

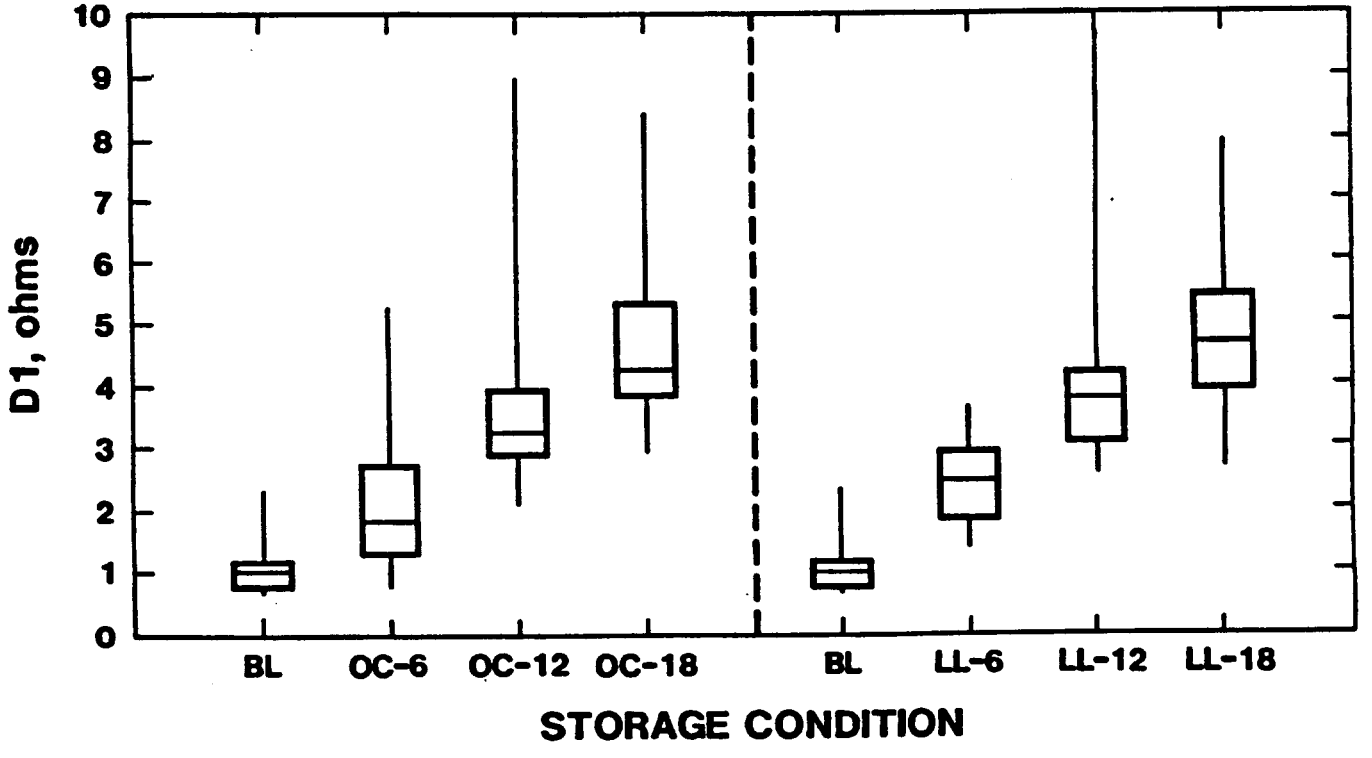

Figure 8. Distribution of D1 values versus storage conditions

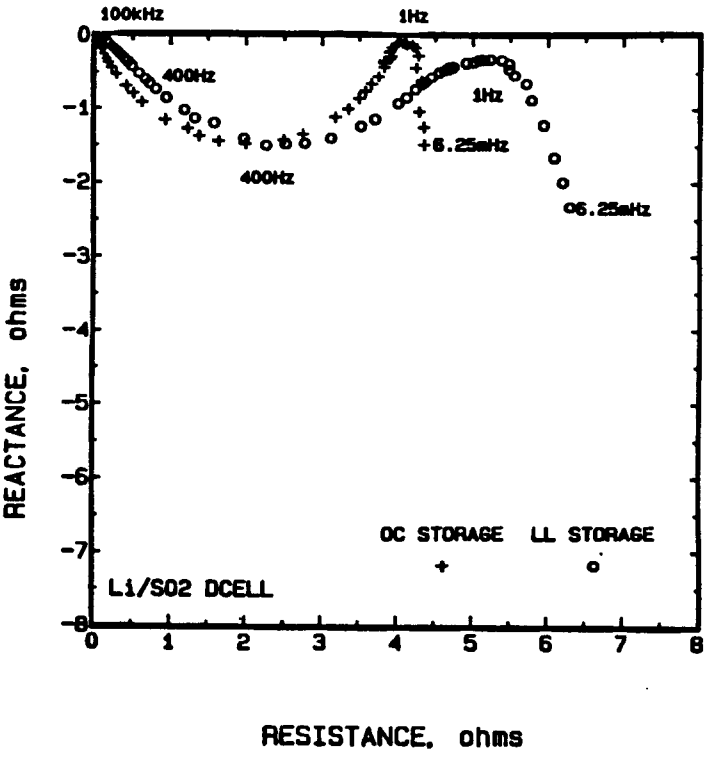

Figure 9. Complex impedance spectrum for OC and LL cells. Storage period was 18 months.

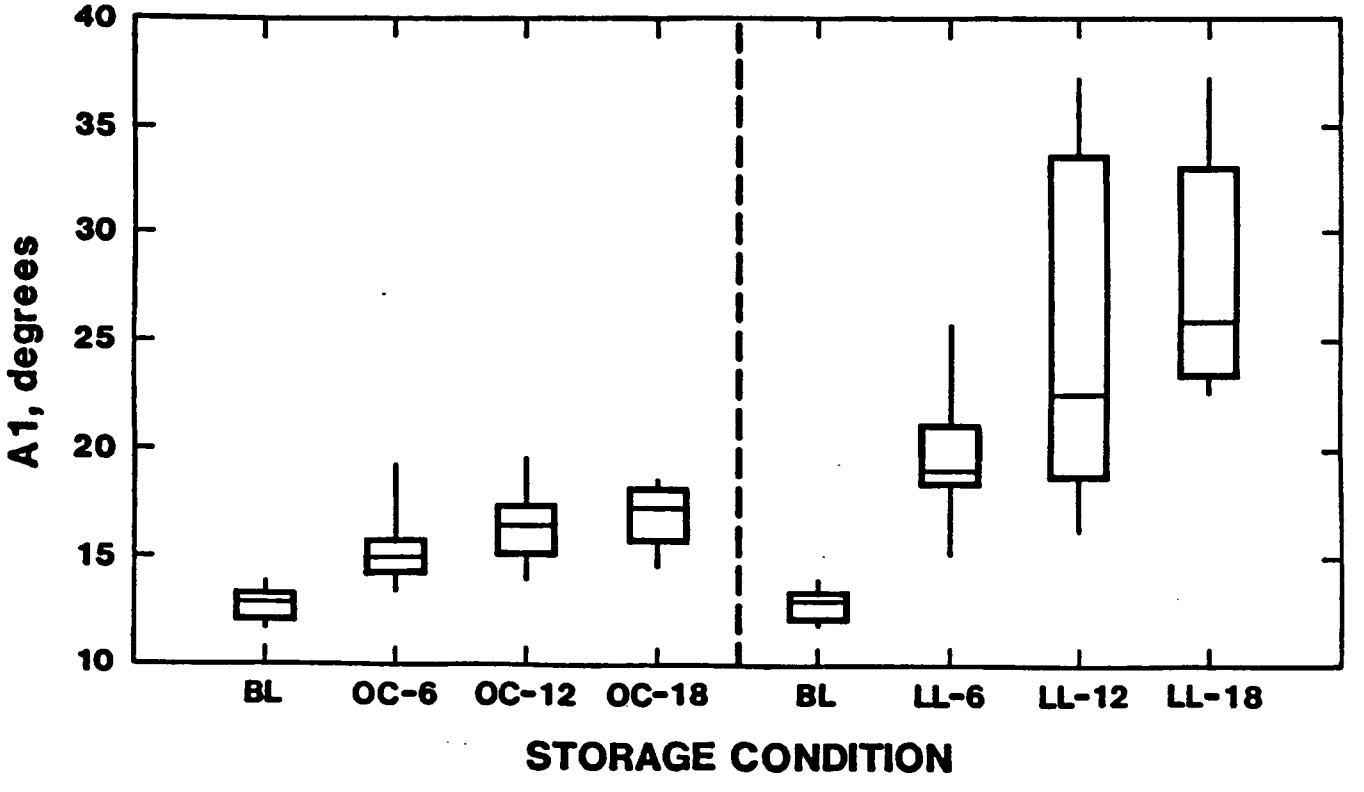

Figure 10. Distribution of A1 values versus storage conditions

The porous carbon cathode collector is represented by an inclined line sometimes called a constant-phase angle. Three variables contribute to the impedance of this element: they are the intercept of the line with the resistance axis, I3; the angle between the line and a line normal to the resistance axis, A3; and the frequency characteristic for that line, F3. Based on laboratory cell measurements, it has been found that the porous carbon cathode collector behaves very much like a semi-infinite linear-pore electrode. The geometric parameters of the porous carbon cathode collector are very important with regard to its contribution to the impedance spectrum and the subsequent discharge behavior. In particular, the discharge of these cells during storage would result in the deposition of a solid product with the porous carbon and affect its mass transport properties. This low-frequency linear region that we associate with the carbon cathode collector is really a part of a very large semicircular component which can be related to the SO_2 reduction on the porous carbon. Because the surface area for the cathode collector is so large and the SO_2 reduction reaction is so slow, the magnitude of this semicircle is very large. Measurements have been performed to as low as 0.0001 Hz, and the semicircle is still not clearly evident. As will be discussed in the following section, although it is known that the carbon cathode collector plays a significant role in the performance of the Li/SO_2 D-cell, no relationship was found between the three measured parameters related to this component and cell performance.

Data Analysis and Cell Screening

The purpose of the data analysis was to identify a subset of nondestructive measurement variables that related empirically with the capacity remaining at the time measurements were made. It is expected that this subset of variables will form a basis for a good predictor of remaining capacity. A good predictor of remaining capacity could then be used to screen cells.

Identification of Relevant Predictors

Correlation analysis (SAND85-1518), segregated by discharge rate, showed that several nondestructive measurement variables related empirically to remaining capacity. The three most significant members of this group are R1, D1, and A1. With some interpretation, Figure 11 illustrates the joint relationship between these variables and remaining capacity as a function of storage regime and discharge rate.

The graphical tool used in these figures is referred to as a glyph. Each symbol represents an individual cell and is composed of a circle representing remaining capacity and three legs representing R1, D1, and A1. The radius of the circle is proportional to the remaining capacity of the represented cell, whereas the lengths of the three legs are proportional to the magnitudes of the three nondestructive measurement variables. The four cells within each storage regime, discharge-load group are arranged positionally in increasing order of remaining capacity (lowest to highest). The positions are: 1 – upper left, 2 – upper right, 3 – lower left, and 4 – lower right.

From these glyph diagrams, one can easily observe the effects of discharge-load and storage regime on capacity. The diameter of the circles generally increases as one proceeds from left to right and bottom to top across the figures. In correspondence to the second of these patterns, notice that the leg sizes generally decrease from bottom to top, especially in the case of the light-load cells. The implication is that R1, D1, and A1 increase with decreasing capacity. These figures serve to illustrate the joint relationship between these measurement variables and capacity. Clearly, there is some predictive relevance jointly contained among these three measurements that enable discrimination between fresh and aged (poorer performing) cells. More subtly, there is a significant pattern within groups of fixed treatment (storage regime and discharge load). There is some correspondence between relative performance within a group of four cells and R1, D1, and A1. In general, performance is inversely related to the length of the legs (values of R1, D1, and A1). Thus, not only is there predictive relevance to allow discrimination between treatment groups, but there is also some predictive relevance within R1, D1, and A1 that allows for discrimination within treatment groups.

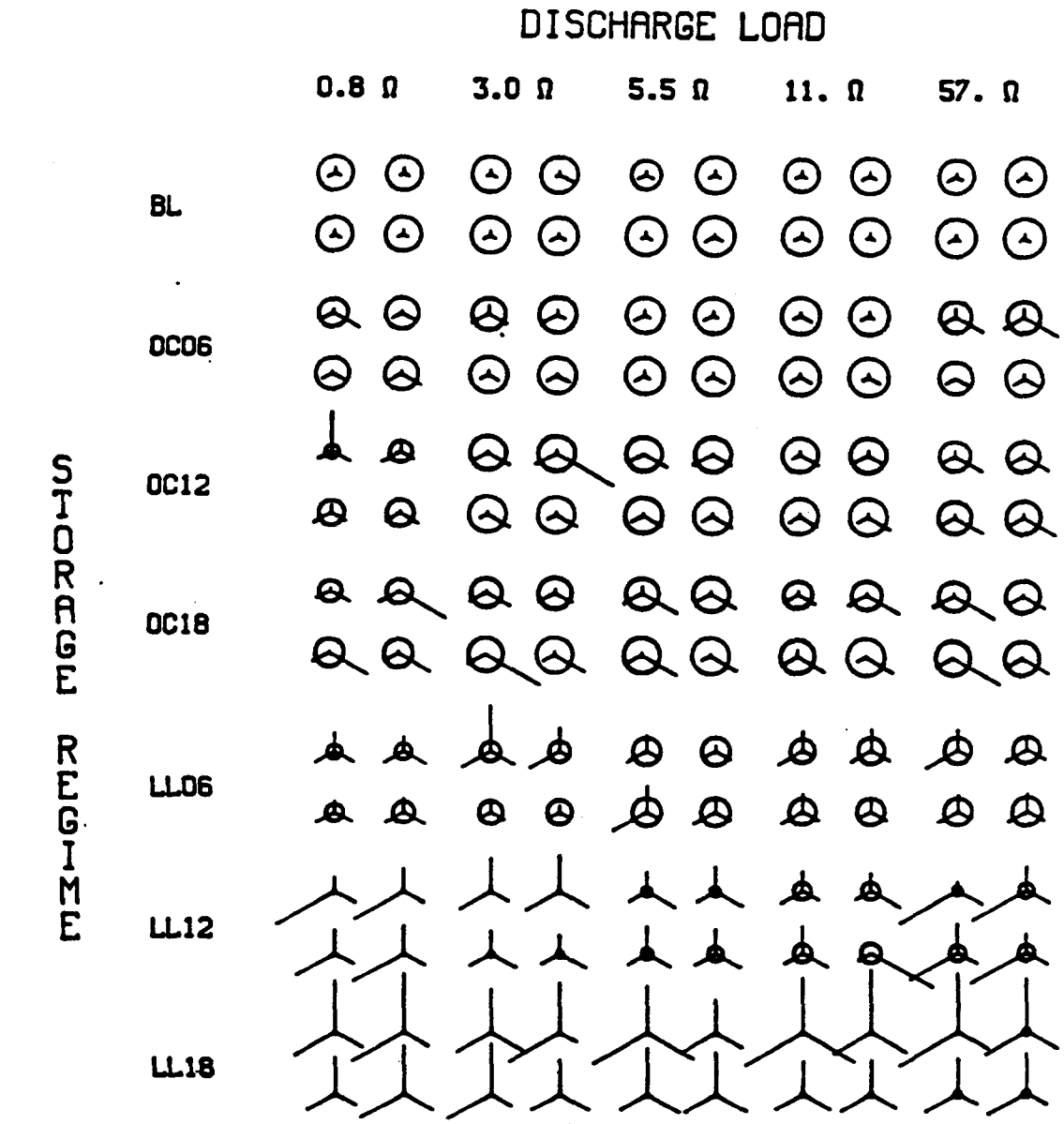

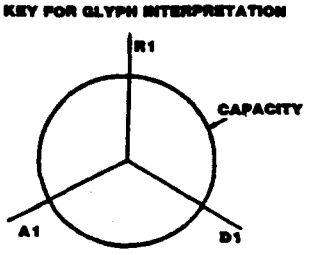

Figure 11. Glyph plot of impedance parameters and remaining capacity

Regression Tree Modeling

In an ideal situation, one would like to model remaining capacity using conventional techniques (e.g., model remaining capacity as a linear combination of the predictor variables). However, this was not possible for a number of reasons, foremost of which is the complexity of the relationship between remaining capacity and the predictor variables. Complexity here refers to the large number of predictor variables and the lack of a linear relationship. Other contributing reasons that reduce the effectiveness of conventional methods include: (1) significant uncertainty in the parameters derived from the complex impedance spectra, and (2) high correlation among the predictor variables. Because of these problems with conventional modeling, regression tree modeling was an attractive approach

Basically, a regression tree model is developed by partitioning the multidimensional space of candidate predictor variables into regions where, within a region, the values of the response variable is similar. This partitioning is accomplished through a series of binary splits of the data set that results in a tree-like structure. The tree consists of a series of logical tests and a set of terminal nodes that define each region.

One complication in the analysis is that performance depends on the discharge rate. To compensate for this, an adjusted value of the remaining capacity was used as the response variable. Table 4 indicates the values used for the various loads.

Table 4. Acceptable capacity for each discharge load

Y = RemCap −	8.50Ah	57 ohm load
	8.25Ah	11 ohm load
	8.00Ah	5.5 ohm load
	7.75Ah	3.0 ohm load
	7.50Ah	0.8 ohm load

DEFINE:

"Good" if $Y \geq 0$

"Bad" if $Y < 0$

The "good" and "bad" criteria are used in Table 5.

For this problem, a computer program called CART (Classification and Regression Trees) supplied by California Statistical Software, Inc., was used to construct a regression tree model using the adjusted values of remaining capacity. CART splits the data set and builds a tree according to certain optimum criteria. (See L. Breiman, T. H. Friedman, R. A. Ohlson, and C. J. Stone, *Classification and Regression Trees*, Wadsworth, Belmont, CA, 1984.) CART constructed a model of normalized capacity based on a set of predictor variables (10 parameters derived from the complex impedance spectrum and open-circuit voltage, OCV) from each of the 140 observations. Figure 12 illustrates the resulting binary tree structure.

The logic used to partition the data set into its terminal nodes, as well as the order of the partitioning, is provided in Figure 12. In addition, a short summary of the terminal node characteristics (n, median, and mad) is also provided. The number of observations that were partitioned into an individual node is "n". The "median" value of Y for observations in a particular node is indicative of the typical performance of cells in that node. The "mad" is the median absolute difference between the observed Y and the median value of Y, for a fixed terminal node. It is reflective of the dispersion in performance within a node.

From Figure 12, it is clear that terminal nodes A and B represent regions in which performance is relatively good (median adjusted performance is >0). Cells in both of these cases had reasonably small values of R1. In node A, cells also had relatively small values for A1. Node B, which was a small step down in performance from node A (median Y = 0.39 versus median Y = 0.67), is characterized by moderate A1 and a relatively high OCV, in addition to a low R1.

Examination of other structures of the regression tree allows for more useful interpretation. Note, for instance, that nodes D and E are different only with respect to A1. Node D cells had relatively small values of A1 and better performance than node E cells. Also note that cells in nodes (F, G) and (H, I) were partitioned by the OCV. Cells in nodes (F, G) had relatively small OCV and correspondingly poorer performance. In summary, interpretation of the regression tree can lead to several general conclusions about the relationship between the nondestructive measurements made and cell performance. Performance seems to be strongly related to R1, A1, and OCV. Good performance is most likely when R1 and A1 are jointly low (node A). The lack of D1 as a splitting variable in the tree structure does not imply that D1 has no predictive relevance by itself. It does imply that D1 adds nothing significant to the prediction ability of the model, given the presence of R1 and A1.

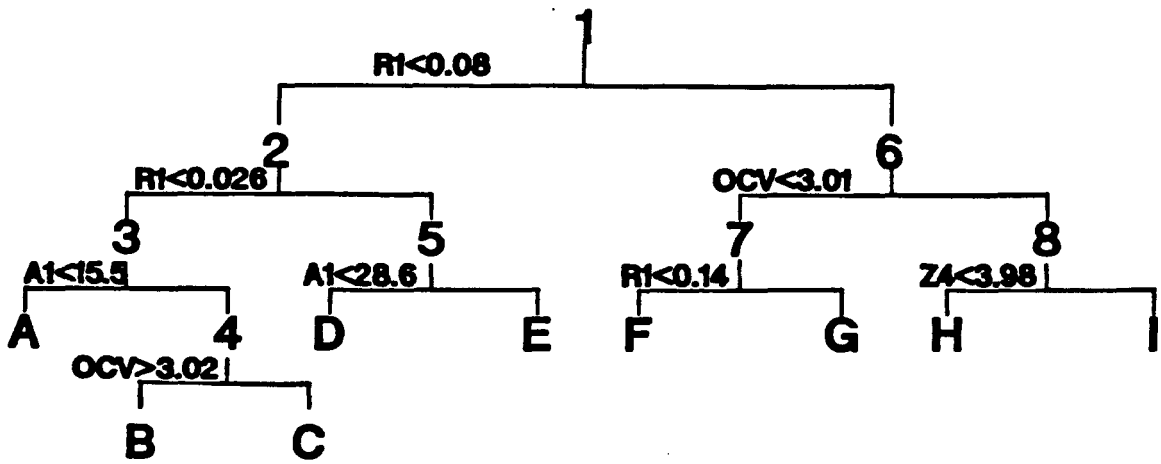

	A	B	C	D	E	F	G	H	I
n	45	9	19	20	2	11	21	7	6
median	.67	.39	-.8	-1.6	-6.4	-5.8	-7.6	-2.6	-4.3
mad	.35	.42	.69	.70	.54	1.0	.23	.64	.94

Figure 12. Regression tree diagram and results from the CART analysis

Cell Screening

From an operational viewpoint, what is needed is an ability to identify those cells with a serious capacity deficiency. A conceptually simple methodology that achieves this is a "decision tree". In the decision tree approach, observed values of important variables, such as R1 and A1, are compared with some threshold values. Each comparison yields a binary response (accept/reject) which corresponds to predicting relatively high or low capacity for the cell. For a cell to be accepted, each comparison must yield an "accept" response, Figure 13. The selected threshold values, X_1 and X_2, would depend upon our previous empirical observations, desired capacity, and the specification of one of two types of risk. Type I risk is defined as the probability of rejecting a cell that, if discharged, would meet the capacity requirements. Type II risk is defined as the probability that a cell that has been accepted will not meet the capacity requirements.

For high-reliability applications, one would select relatively low target values for Type II risk. This implies the selection of relatively stringent threshold values which generally imply relatively large Type I risk. So, as we require higher reliability, we would generally reject more "good" cells. Therefore, the problem is to find relevant variables and a set of threshold values that both minimize Type II risk yet do not make the Type I risk unacceptably large. CART selects the optimal set of prediction variables and threshold values, given an existing data set and a specification of relative risk (Type I/Type II). In addition, CART provides accurate estimates of the risks associated with the set of prediction variables and threshold values.

In view of the CART results, it seems reasonable that R1 and A1 could be used in tandem to effect a screen that could separate cells that have seen some destructive storage from cells that have not. This could arise in a situation in which cells have been exposed to a variety of unknown environments and then are subsequently tested to determine their condition. If the condition were judged to be relatively bad, based on R1 and A1 values, then they would not be used. Otherwise, they would be used. This would effectively improve the reliability of the cells that were ultimately used.

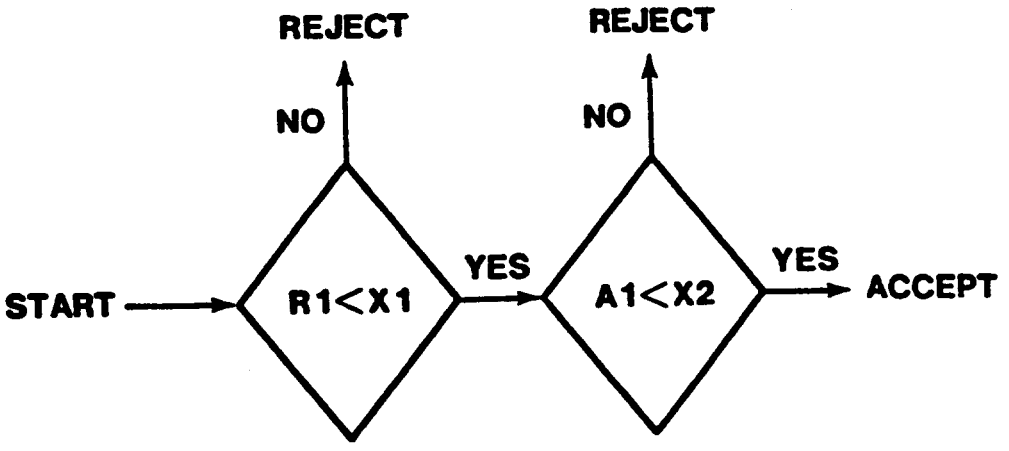

Figure 13. Decision tree for cell acceptance. R1 and A1 are impedance parameters. X_1 and X_2 are selected threshold values.

The mechanics of such a screen would be simple. First, measure R1 and A1. Accept the cell only if R1 $<$ 0.026 and A1 $<$ 15.5 for that cell. If, within a storage regime, discharge-load group, some cells passed and some cells failed, the screen generally rejected the poorer performing cells. Again, this has some practical importance because it indicates that this screening technique could separate poor performing cells in a group of cells that had seen equivalent treatment. Table 5 summarizes the results using the above criteria and the remaining capacity for the SM cells. (The values for "good" and "bad" cells were defined in Table 4.)

Table 5. Summary of regression tree screening results from the CART analysis

	Total	# Rejected	# Accepted
"Good" Cells	51	4	47
"Bad" Cells	89	82	7
Total	140	86	54

Passed cells only from nodes A and B

Conclusions

In summary, interpretation of the regression tree leads to several general conclusions about the relationship between nondestructive measurements made and cell performance. Performance seems to be strongly related to R1 and A1. Good performance is most likely when both R1 and A1 are jointly low. In view of these results, it seems reasonable that R1 and A1 could be used in tandem to effect a screen that could separate cells that have seen some destructive storage from cells that have not. This could arise in a situation in which cells have been exposed to a variety of unknown environments and then are subsequently tested to determine their condition. If the condition of the cell was judged to be relatively bad, based on R1 and A1 values, then the cell would be rejected. Otherwise it would be used. This screen would effectively improve the reliability of the cells that were ultimately used.

While the idea of using a decision tree to screen cells appears to be valid for this particular lot, there are several remaining questions. First of all, do R1 and A1 have predictive relevance over all lots of this design of cell? If so, would the critical values for the screening purposes (e.g., 0.026 and 15.5) be dependent on the lot? The general applicability of this screening technique depends on the answer to the above questions. To answer these questions, additional studies of cells from a variety of lots will have to be performed.

Based on the results from this program, it appears that cell parameters derived from nondestructive measurements such as complex impedance analysis could be used to effect a cell screening tree. Except for a few instances where the heat flux from "bad" cells was very large, microcalorimetry did not show any correlation with cell performance.

APPENDIX A

Report Background Publications List

S. C. Levy, N. H. Hall, F. M. Delnick, and C. D. Jaeger, *Predicting Battery Reliability Annual Report, May 1981 - April 1982*, SAND82-1938, Sandia National Laboratories, Albuquerque, NM.

C. D. Jaeger, N. H. Hall, and S. C. Levy, *Predicting Battery Reliability, Second Annual Report, May 1982 - April 1983*, SAND83-2474, Sandia National Laboratories, Albuquerque, NM.

C. D. Jaeger, N. H. Hall, and E. V. Thomas, *Lithium Ambient-Temperature Battery Reliability Program, May 1983 - April 1985*, SAND85-1518, Sandia National Laboratories, Albuquerque, NM.

C. D. Jaeger, S. C. Levy, E. V. Thomas, and J. T. Cutchen, "Studies of High Reliability Long-Life Li/SO_2 Cells," *J. Power Sources*, 20, 27 (1987).

C. D. Jaeger, "Improved Li/SO_2 Cell Reliability Using Complex Impedance Analysis," *Proc. of the Symposium on Lithium Batteries*, 87-1, 93 (1987).

E. V. Thomas, C. D. Jaeger, and S. C. Levy, "Improving Battery Reliability by Using Regression Trees," *Proc. of 3rd Annual Battery Conference.*

C. D. Jaeger and J. C. D'Angelo, "The Use of Complex Impedance Analysis in Predicting Reliability of Li/SO_2 Primary Cells," *ECS Extended Abstracts*, 83-1, 47 (1983).

C. D. Jaeger and N. H. Hall, "Sandia National Laboratories' Battery Reliability Program," *ECS Extended Abstracts*, 84-2, 569 (1984).

C. D. Jaeger and E. V. Thomas, "Spline Fit to Complex Impedance Data," *ECS Extended Abstracts*, 85-2 (1985).

APPENDIX B

SM Cell Parameters After Storage

#	I3	F3	A3	R1	F1	D1	A1	F2	D2	A2	OCV	Rem CAP	Pulse Min	Load	Cord1	Cord2	Heat	Wt	Desc
2	1.133	0.0068	5.8	0.0160	232.9	0.996	13.9	4.98	0.223	35.3	2.9979	9.03	2.886	57.0	0.967	0.182	0	0.00	BL00B
3	1.050	0.0081	7.5	0.0216	340.0	0.894	12.0	1.56	0.203	28.4	2.9891	9.32	2.876	57.0	0.875	0.178	0	0.00	BL00B
4	1.073	0.0084	5.0	0.0183	249.8	1.041	14.6	3.18	0.198	37.7	2.9989	8.13	2.881	57.0	1.007	0.156	0	0.00	BL00B
5	1.447	0.0056	4.8	0.0173	210.9	1.265	13.5	3.49	0.300	28.9	2.9966	8.89	2.642	11.0	1.230	0.263	0	0.00	BL00B
6	0.937	0.0092	5.9	0.0200	377.9	0.785	11.5	1.84	0.273	36.6	2.9882	8.90	2.656	11.0	0.769	0.219	0	0.00	BL00B
7	1.043	0.0087	5.3	0.0189	249.2	1.009	14.0	3.72	0.293	33.9	3.0006	8.69	2.656	11.0	0.979	0.243	0	0.00	BL00B
8	1.006	0.0081	4.7	0.0232	361.2	0.819	13.0	1.50	0.323	27.8	2.9923	7.96	2.656	11.0	0.790	0.285	0	0.00	BL00B
10	0.926	0.0098	7.2	0.0245	345.3	0.819	12.1	1.92	0.147	31.0	2.9867	8.18	2.212	0.8	0.800	0.126	0	0.00	BL00B
11	1.293	0.0072	7.9	0.0200	319.4	1.028	12.0	1.64	0.332	32.9	2.9863	8.21	2.212	0.8	1.006	0.279	0	0.00	BL00B
12	0.803	0.0107	5.0	0.0198	380.3	0.735	12.6	1.34	0.130	33.2	2.9842	8.29	2.202	0.8	0.717	0.108	0	0.00	BL00B
13	0.931	0.0095	4.6	0.0212	335.1	0.802	13.1	1.74	0.170	29.2	2.9870	8.82	2.544	5.5	0.782	0.149	0	0.00	BL00B
14	1.481	0.0059	4.5	0.0186	239.6	1.178	14.0	4.48	0.538	45.0	2.9960	6.92	2.510	5.5	1.143	0.380	0	0.00	BL00B
15	1.440	0.0059	0.6	0.0134	218.2	1.283	14.7	2.18	0.220	31.7	2.9967	9.29	2.505	5.5	1.241	0.187	0	0.00	BL00B
16	1.389	0.0061	8.7	0.0216	323.2	1.028	12.1	1.44	0.555	34.8	2.9893	9.14	2.485	5.5	1.005	0.456	0	0.00	BL00B
17	1.112	0.0077	9.4	0.0195	334.7	0.977	11.9	1.83	0.187	30.2	2.9880	8.61	2.417	3.0	0.956	0.162	0	0.00	BL00B
18	2.904	0.0028	4.8	0.0160	144.7	2.348	11.7	1.93	0.860	32.5	2.9875	8.64	2.388	3.0	2.299	0.726	0	0.00	BL00B
19	1.324	0.0068	3.8	0.0157	224.7	1.153	14.2	2.13	0.282	35.9	2.9916	8.91	2.441	3.0	1.117	0.228	0	0.00	BL00B
20	0.914	0.0095	7.4	0.0195	340.2	0.814	13.2	1.88	0.144	25.0	2.9833	8.76	2.461	3.0	0.793	0.130	0	0.00	BL00B
21	2.052	0.0041	1.7	0.0154	147.7	1.769	13.4	2.02	0.447	35.3	3.0040	8.92	2.582	11.0	1.721	0.365	0	80.86	OC06P
22	0.923	0.0104	7.7	0.0223	246.5	0.807	14.1	3.27	0.135	27.7	3.0108	9.01	2.697	11.0	0.783	0.120	0	81.29	OC06P
23	2.040	0.0041	0.0	0.0165	153.6	1.727	13.1	1.76	0.629	38.7	2.9987	9.19	2.594	11.0	1.682	0.498	0	80.92	OC06P
24	1.877	0.0057	3.6	0.0143	149.3	1.732	14.8	1.68	0.196	16.0	3.0012	9.05	2.605	11.0	1.675	0.188	0	80.86	OC06P
25	1.832	0.0054	4.7	0.0184	202.4	1.589	14.0	2.56	0.431	29.9	3.0130	8.69	2.412	3.0	1.541	0.374	0	84.48	OC06P
26	2.828	.0026	11.6	0.0386	126.0	2.828	17.8	1.18	0.120	7.7	2.9883	7.71	2.312	3.0	2.685	0.119	0	83.60	OC06P
27	1.284	0.0066	9.7	0.0220	226.6	1.174	17.3	1.79	0.163	24.0	3.0082	8.63	2.440	3.0	1.121	0.149	0	80.73	OC06P
28	2.511	0.0033	3.8	0.0078	154.0	2.000	14.9	1.45	0.369	0.0	3.0132	8.71	2.436	3.0	1.932	0.369	0	81.09	OC06P
29	1.992	0.0041	6.4	0.0160	195.0	1.731	13.4	2.15	0.426	30.3	3.0193	9.19	2.513	5.5	1.684	0.368	0	81.43	OC06P
30	0.755	0.0116	4.5	0.0205	272.9	0.684	14.6	2.34	0.099	34.8	3.0079	8.74	2.617	5.5	0.662	0.081	0	81.01	OC06P
31	0.887	0.0099	5.3	0.0232	245.8	0.803	15.2	2.19	0.098	26.0	3.0047	8.61	2.601	5.5	0.775	0.089	0	80.78	OC06P
32	0.883	0.0102	1.7	0.0238	234.8	0.853	14.7	9.00	0.059	9.3	3.0028	8.87	2.597	5.5	0.825	0.058	0	80.89	OC06P
33	4.042	.0017	12.3	0.0160	132.2	3.510	15.1	0.03	1.234	35.4	3.0212	8.74	2.494	11.0	3.388	1.007	0	0.00	OC12P
34	2.184	0.0027	3.0	0.0220	190.4	2.162	17.2	0.18	0.150	23.1	3.0165	8.43	2.590	11.0	2.065	0.138	0	0.00	OC12P
35	3.213	0.0022	6.3	0.0167	153.0	2.879	13.7	0.58	0.696	33.3	3.0277	8.34	2.535	11.0	2.796	0.582	0	0.00	OC12P
36	2.992	0.0026	5.6	0.0140	136.1	2.816	15.0	0.43	0.415	31.3	3.0168	8.49	2.534	11.0	2.720	0.354	0	0.00	OC12P
37	4.116	0.0019	1.5	0.0000	141.0	3.642	16.0	0.21	0.965	40.3	3.0285	8.30	2.330	5.5	3.487	0.737	0	0.00	OC12P
38	3.026	0.0027	1.1	0.0053	162.7	2.890	19.1	0.19	0.542	45.0	3.0228	8.39	2.415	5.5	2.731	0.383	0	0.00	OC12P
39	3.493	0.0023	3.5	0.0140	141.0	3.136	15.0	0.76	0.393	31.4	3.0257	8.65	2.386	5.5	3.029	0.336	0	0.00	OC12P
40	3.214	0.0024	6.4	0.0091	152.1	2.883	15.6	0.41	0.491	31.7	3.0283	8.62	2.400	5.5	2.777	0.418	0	0.00	OC12P
41	3.103	.0030	11.5	0.0963	203.0	2.865	19.3	1.16	0.580	30.3	3.0131	6.18	2.538	11.0	2.703	0.501	0	80.23	LL06P
42	2.977	0.0032	9.5	0.0492	180.9	2.507	14.8	1.15	0.699	33.9	2.9883	6.44	2.570	11.0	2.425	0.580	0	81.16	LL06P
43	1.488	0.0069	7.3	0.0871	248.9	1.321	21.4	1.14	0.142	31.1	3.0117	5.67	2.658	11.0	1.230	0.121	0	80.08	LL06P
44	3.634	.0025	10.4	0.0792	232.8	2.525	19.6	1.41	0.667	26.1	3.0136	6.25	2.553	11.0	2.379	0.599	0	80.79	LL06P
45	2.595	.0031	13.5	0.0685	213.2	2.366	20.1	1.68	0.317	20.5	3.0144	6.72	2.427	5.5	2.223	0.297	0	80.95	LL06P
46	2.698	0.0031	6.1	0.0262	194.1	2.321	15.5	1.44	0.693	36.6	3.0124	6.56	2.482	5.5	2.237	0.557	0	81.31	LL06P
47	2.473	0.0039	7.3	0.0789	279.4	2.046	18.9	1.29	0.668	38.9	3.0151	6.45	2.436	5.5	1.936	0.520	0	80.60	LL06P
48	1.896	0.0057	7.4	0.1164	299.4	1.785	25.9	0.67	0.158	27.9	3.0159	6.66	2.483	5.5	1.606	0.140	0	80.05	LL06P
49	1.785	0.0055	8.3	0.1087	286.9	1.636	23.9	1.32	0.236	29.2	3.0152	4.91	2.351	3.0	1.496	0.286	0	80.49	LL06P
50	1.776	0.0055	6.0	0.0299	197.1	1.622	15.2	1.76	0.219	26.5	3.0101	5.79	2.403	3.0	1.566	0.196	0	80.98	LL06P
51	2.319	0.0040	7.2	0.0405	166.7	2.133	15.2	2.00	0.285	23.2	3.0102	5.51	2.344	3.0	2.058	0.262	0	81.16	LL06P
52	3.728	.0025	10.6	0.2100	259.0	3.707	23.2	0.73	0.197	8.7	3.0150	4.64	2.052	3.0	3.407	0.195	0	79.91	LL06P
53	3.611	0.0024	2.2	0.0140	185.8	3.292	13.9	0.40	0.552	40.8	3.0101	8.59	2.268	3.0	3.196	0.418	0	0.00	OC12P
54	9.122	.0010	15.0	0.0156	92.6	8.960	19.7	1.97	0.600	20.1	2.9987	8.53	1.736	3.0	8.436	0.563	0	0.00	OC12P
55	3.565	0.0023	8.1	0.0093	144.4	3.504	16.4	0.89	0.443	27.7	3.0218	8.29	2.156	3.0	3.362	0.393	0	0.00	OC12P
56	4.225	0.0021	0.0	0.0131	184.9	3.540	13.8	0.35	1.115	45.0	3.0128	8.55	2.246	3.0	3.438	0.788	0	0.00	OC12P
57	2.999	0.0029	0.6	0.0178	188.0	2.793	16.3	0.43	0.622	45.0	3.0285	6.66	2.531	11.0	2.681	0.440	0	0.00	OC18P
58	3.583	0.0025	7.3	0.0057	189.5	4.218	14.3	0.55	0.340	16.9	3.0224	8.78	2.493	11.0	4.079	0.326	0	0.00	OC18P
59	4.176	0.0021	6.2	0.0301	148.1	4.170	17.4	0.36	0.188	8.7	3.0201	7.94	2.476	11.0	3.980	0.188	0	0.00	OC18P
60	5.055	0.0019	0.0	0.0114	147.4	5.076	18.5	0.32	0.339	18.3	3.0188	7.04	2.425	11.0	4.814	0.322	0	0.00	OC18P
61	3.908	0.0023	3.2	0.0160	165.0	3.904	16.8	0.17	0.251	21.3	3.0291	8.39	2.256	5.5	3.737	0.234	0	0.00	OC18P

#	I3	F3	A3	R1	F1	D1	A1	F2	D2	A2	OCV	Rem CAP	Pulse Min	Load	Cord1	Cord2	Heat	Wt	Desc
62	5.425	0.0015	5.7	0.0121	118.2	5.392	16.4	0.29	0.382	28.9	3.0278	0.39	2.205	5.5	5.173	0.334	0	0.00	OC18P
63	5.458	0.0018	3.1	0.0344	147.0	5.388	18.6	0.17	0.406	27.3	3.0220	7.62	2.252	5.5	5.108	0.361	0	0.00	OC18P
64	4.312	0.0020	4.6	0.0068	111.9	4.056	14.2	0.35	0.405	27.0	3.0201	0.66	2.362	5.5	3.932	0.361	0	0.00	OC18P
65	2.052	0.0030	3.9	0.0200	190.6	2.001	17.5	0.44	0.267	27.9	3.0235	7.75	2.250	3.0	2.672	0.236	0	0.00	OC18P
66	4.352	0.0023	0.0	0.0166	118.2	4.672	15.4	0.20	0.692	35.4	3.0177	0.37	2.102	3.0	4.504	0.564	0	0.00	OC18P
67	9.092	0.0011	0.7	0.0000	115.2	0.453	18.2	0.29	1.090	45.0	2.9991	7.94	1.041	3.0	0.030	1.336	0	0.00	OC18P
68	3.810	0.0022	5.3	0.0110	173.0	3.750	17.5	0.32	0.270	19.3	3.0278	7.19	2.140	3.0	3.577	0.254	0	0.00	OC18P
69	2.598	0.0037	2.0	0.0087	240.3	2.488	20.1	0.12	0.529	43.3	3.0113	4.03	2.605	11.0	2.336	0.385	0	0.00	LL12P
70	4.947	0.0020	7.4	0.0010	154.7	4.688	17.2	0.60	0.899	39.2	3.0119	4.09	2.558	11.0	4.394	0.697	0	0.00	LL12P
71	4.283	0.0025	9.9	0.1186	250.0	3.919	18.6	0.34	0.546	36.9	3.0133	4.17	2.530	11.0	3.714	0.436	0	0.00	LL12P
72	4.371	.0016	43.0	0.0000	111.7	9.794	15.9	0.20	3.965	39.3	3.0135	4.63	2.535	11.0	9.419	3.068	0	0.00	LL12P
73	4.247	0.0040	0.0	0.1076	262.2	3.910	19.0	0.30	0.410	21.5	3.0039	3.37	2.302	5.5	3.670	0.389	0	0.00	LL12P
74	3.701	0.0029	7.4	0.1209	265.3	3.641	19.0	0.33	0.324	27.7	3.0040	2.52	2.377	5.5	3.443	0.286	0	0.00	LL12P
75	5.140	0.0020	7.9	0.1125	247.5	4.232	18.9	0.24	0.353	16.5	3.0081	2.22	2.317	5.5	4.003	0.339	0	0.00	LL12P
76	4.424	0.0025	5.6	0.0089	236.1	4.304	18.3	0.25	0.590	34.6	3.0186	2.19	2.326	5.5	4.163	0.492	0	0.00	LL12P
77	2.805	0.0039	9.5	0.1517	354.5	2.606	24.9	0.49	0.357	36.4	3.0106	0.37	2.230	3.0	2.436	0.288	0	0.00	LL12P
78	4.803	0.0027	7.8	0.0825	245.4	4.005	18.6	0.37	0.258	15.1	3.0084	1.55	2.167	3.0	3.797	0.249	0	0.00	LL12P
79	4.118	0.0027	0.4	0.1023	263.1	3.918	20.2	0.20	0.600	34.4	3.0022	1.13	2.150	3.0	3.670	0.495	0	0.00	LL12P
80	4.417	.0022	12.3	0.1633	205.0	4.393	25.9	0.40	0.477	32.4	3.0070	0.63	2.057	3.0	3.950	0.402	0	0.00	LL12P
81	4.127	.0024	24.7	0.1571	320.0	3.802	24.0	0.76	0.926	45.0	3.0057	0.61	2.532	11.0	3.547	0.655	0	0.00	LL18P
82	6.349	.0018	13.5	0.2042	267.4	5.544	27.7	0.36	2.072	45.0	3.0148	0.49	2.392	11.0	4.907	1.465	0	0.00	LL18P
83	4.957	.0023	20.4	0.1521	314.9	4.273	22.6	0.89	1.435	45.0	3.0046	0.60	2.536	11.0	3.945	1.014	0	0.00	LL18P
84	7.917	.0014	19.3	0.2459	330.3	8.045	37.4	0.79	0.719	21.9	3.0036	0.19	2.138	11.0	6.398	0.667	0	0.00	LL18P
85	6.088	.0018	15.5	0.1940	276.3	4.849	24.6	1.51	2.348	45.0	3.0053	0.39	1.986	5.5	4.410	1.661	0	0.00	LL18P
86	4.274	.0022	27.7	0.1493	339.6	4.088	25.9	0.27	0.993	45.0	3.0056	0.34	2.049	5.5	3.670	0.702	0	0.00	LL18P
87	5.941	.0019	21.7	0.2152	262.8	4.962	22.4	1.45	2.012	45.0	3.0034	0.34	1.932	5.5	4.588	1.423	0	0.00	LL18P
88	5.479	.0021	22.9	0.2116	321.0	7.177	35.7	1.18	0.807	21.6	3.0046	0.04	1.925	5.5	5.030	0.750	0	0.00	LL18P
89	4.926	.0025	16.0	0.1611	326.6	4.473	23.3	0.57	1.154	45.0	2.9967	0.11	1.986	3.0	4.107	0.816	0	0.00	LL18P
90	2.628	.0058	16.2	0.2267	393.9	2.576	33.8	0.44	0.303	21.4	2.9966	0.05	2.049	3.0	2.148	0.282	0	0.00	LL18P
91	5.924	.0020	11.3	0.1984	267.4	4.943	25.9	0.28	1.075	45.0	2.9993	0.01	1.932	3.0	4.445	1.326	0	0.00	LL18P
92	3.399	.0042	19.6	0.2311	405.9	3.128	30.7	0.67	0.636	28.6	2.9958	0.05	1.925	3.0	2.683	0.558	0	0.00	LL18P
93	5.921	0.0015	6.7	0.0369	184.2	5.316	19.3	0.88	0.659	20.8	3.0031	7.69	2.755	57.0	5.017	0.616	15	0.00	OC06P
94	2.449	0.0034	6.6	0.0216	152.4	2.147	15.4	1.91	0.425	30.2	3.0164	0.58	2.072	57.0	2.070	0.367	17	0.00	OC06P
95	4.690	0.0017	2.3	0.0393	122.1	4.202	16.4	0.79	0.681	26.6	3.0055	7.45	2.795	57.0	4.031	0.609	24	0.00	OC06P
96	2.119	0.0043	3.4	0.0000	165.0	1.935	15.2	2.31	0.347	20.0	3.0172	7.77	2.074	57.0	1.860	0.306	19	0.00	OC06P
97	4.582	0.0010	7.2	0.0101	120.4	4.104	15.6	0.69	0.692	31.8	3.0114	6.85	1.912	0.0	3.952	0.588	19	0.00	OC06P
98	3.419	.0018	18.6	0.0158	158.7	3.068	15.4	1.57	0.464	24.9	3.0149	7.74	1.999	0.0	2.958	0.421	21	0.00	OC06P
99	1.993	0.0041	7.0	0.0110	160.7	1.844	14.9	2.08	0.313	27.5	3.0190	7.78	2.187	0.0	1.781	0.270	20	0.00	OC06P
100	2.838	0.0033	0.0	0.0000	160.5	2.255	14.6	1.24	0.959	43.0	3.0206	7.68	2.023	0.0	2.183	0.781	15	0.00	OC06P
101	2.828	0.0036	4.0	0.0786	261.3	2.684	18.7	1.17	0.363	29.3	3.0046	6.07	2.034	57.0	2.843	0.317	24	0.00	LL06P
102	2.588	.0037	11.1	0.0749	262.3	2.647	18.9	1.69	0.702	27.5	3.0037	6.42	2.050	57.0	1.936	0.622	18	0.00	LL06P
103	3.226	0.0032	0.0	0.0592	241.2	2.891	19.6	0.79	0.657	45.0	3.0068	6.24	2.038	57.0	2.722	0.465	25	0.00	LL06P
104	1.573	0.0060	5.7	0.0937	389.2	1.376	24.8	0.72	0.288	38.3	3.0134	6.28	2.097	57.0	1.249	0.249	21	0.00	LL06P
105	3.431	0.0028	7.3	0.0520	256.8	2.701	18.5	1.59	0.482	29.5	3.0094	4.09	1.833	0.0	2.562	0.419	14	0.00	LL06P
106	3.614	0.0027	5.7	0.0618	230.6	3.308	18.4	0.88	0.618	37.7	3.0101	5.07	1.848	0.0	3.138	0.489	18	0.00	LL06P
107	0.000	0.0000	0.0	0.0649	221.0	3.434	19.1	0.89	1.118	44.9	3.0115	3.86	1.771	0.0	3.244	0.792	20	0.00	LL06P
108	1.512	.0067	18.5	0.0859	230.4	2.925	18.9	1.36	0.335	25.1	3.0105	3.39	1.796	0.0	2.766	0.383	14	0.00	LL06P
125	4.979	0.0015	7.9	0.0212	108.4	5.038	17.3	0.81	0.452	1.1	3.0071	7.96	2.721	57.0	4.089	0.452	27	0.00	OC12P
126	4.340	0.0019	0.6	0.0154	110.6	3.974	16.2	0.39	1.047	45.0	3.0153	7.46	2.764	57.0	3.816	0.748	13	0.00	OC12P
127	4.471	0.0020	0.8	0.0236	115.5	4.298	15.3	0.27	1.078	45.0	3.0158	7.24	2.751	57.0	4.147	0.762	15	0.00	OC12P
128	4.782	0.0021	0.0	0.0173	115.9	4.412	16.9	0.26	0.733	37.3	3.0148	7.69	2.742	57.0	4.221	0.583	16	0.00	OC12P
129	3.349	0.0026	2.4	0.0098	141.4	2.867	16.4	1.00	0.495	36.6	3.0178	6.32	1.858	0.0	2.758	0.398	16	0.00	OC12P
130	4.465	.0020	11.2	0.5301	133.4	2.824	16.3	0.30	1.258	33.2	3.0186	3.20	1.649	0.0	2.718	1.052	14	0.00	OC12P
131	2.382	0.0048	3.4	0.0343	151.8	2.357	18.3	0.45	0.247	22.9	3.0013	5.89	1.748	0.0	2.230	0.227	33	0.00	OC12P
132	2.178	0.0044	6.3	0.0328	186.8	2.015	18.7	0.85	0.348	39.0	3.0047	5.21	1.688	0.0	1.908	0.271	32	0.00	OC12P
133	3.207	0.0032	9.2	0.1092	343.8	3.591	35.0	0.25	0.241	23.3	3.0045	3.43	2.794	57.0	2.941	0.221	30	0.00	LL12P
134	2.859	0.0037	3.6	0.0026	389.4	3.264	36.2	0.03	0.473	32.9	3.0051	3.68	2.811	57.0	2.635	0.397	25	0.00	LL12P
135	3.531	0.0030	8.4	0.0416	410.1	3.904	37.4	0.30	0.763	45.0	3.0052	2.88	2.776	57.0	3.101	0.548	26	0.00	LL12P
136	2.752	.0041	13.0	0.1305	340.3	3.046	32.5	0.27	0.094	5.7	3.0047	3.64	2.818	57.0	2.567	0.093	19	0.00	LL12P
137	2.748	0.0040	9.9	0.0662	514.1	3.130	37.2	0.15	0.323	36.4	3.0061	0.00	1.882	0.0	2.501	0.260	29	0.00	LL12P
138	2.752	0.0041	9.9	0.1048	361.8	3.011	33.1	0.29	0.181	19.7	3.0076	0	1.126	0.0	2.523	0.170	25	0.00	LL12P
139	2.821	.0041	10.8	0.1072	310.5	2.906	28.1	0.29	0.232	22.7	3.0051	0	1.483	0.0	2.564	0.214	28	0.00	LL12P
140	2.979	0.0035	8.2	0.1232	413.2	3.223	33.8	0.12	0.484	36.7	3.0051	0	1.127	0.0	2.679	0.324	25	0.00	LL12P

DISTRIBUTION:

8 Hughes Aircraft Co.
Power Sources Dept.
Attn: E. J. Stofel, S41/A315
PO Box 92919
Los Angeles, CA 90009

2 Honeywell
Power Sources Center
Attn: D. Chua
R. Barnabei
104 Rock Road
Horsham, PA 19044

1 Jet Propulsion Laboratory
Attn: G. Halpert
4800 Oak Grove Drive
Pasadena, CA 91109-8099

1 The Aerospace Corp.
Attn: H. F. Bittner
2350 E. El Segundo Blvd.
PO Box 92957
El Segundo, CA 90009

1 Altus Corp.
1610 Crane Court
San Jose, CA 95112

1 Boeing Aerospace Co.
Attn: C. J. Johnson
PO Box 3999
Seattle, WA 98124-2499

1 Eagle Picher Industries
Electronics Division
Attn: R. Higgins
PO Box 47
Joplin, MO 64802

1 Electrochem Industries
Attn: W. D. K. Clark
10000 Wehrle Drive
Clarence, NY 14031

1 Eveready Battery Co.
Attn: G. Blomgren
25225 Detroit Rd.
PO Box 45035
Westlake, OH 44145

6 General Electric Co.
Neutron Devices Dept.
Attn: R. Antepenko
W. C. Brown
B. J. Mincey
T. P. Evans
J. D. Sgro
C. G. Wagner
PO Box 2908
Largo, FL 34294-2908

5 Roy H. Kissinger
15004 Native Dancer Rd.
Gaithersburg, MD 20878

1 Power Conversion Inc.
Attn: J. Barrella
495 Boulevard
Elmwood Park, NJ 07407

1 SAFT America
Attn: N. S. Raman
107 Beaver Court
Cockeysville, MD 21030

2 Tracor JITCO Battery Tech Ctr.
Attn: N. Margalit
C. R. Walk
1601 Research Blvd.
Rockville, MD 20850

3 USALABCOM
ETDL
SLCET-PB (M. Brundage)
(E. Reiss)
SLCET-PR (M. Binder)
Fort Monmouth, NJ 07703-5000

3 Naval Surface Warfare Center
Code R-33
Attn: J. A. Barnes
P. Davis
W. Kilroy
Silver Spring, MD 20910

1 Naval Weapons Support Center
Code 3054
Attn: S. Shuler
Crane, IN 47522

DISTRIBUTION (Continued):

4 Whittaker-Yardney Power Systems
Attn: R. S. Wissoker
G. H. Boyle
F. Goebel
R. McDonald
520 Winter Street
Waltham, MA 02154

1 Electrochemical Science & Tech Ctr.
University of Ottawa
Attn: G. Donaldson
32 George Glinski
Ottawa, Ontario
KIN 6N5 CANADA

1	2500	R. L. Schwoebel
1	2520	N. J. Magnani
1	2522	R. P. Clark
10	2523	J. Q. Searcy
1	2523	A. R. Baldwin
1	2523	D. A. Bouchard
1	2523	W. R. Cieslak
1	2523	C. C. Crafts
1	2523	F. M. Delnick
10	2523	S. C. Levy
1	2523	H. K. Street
1	2525	R. B. Diegle
1	2526	P. C. Butler
5	5245	C. D. Jaeger
1	7223	R. G. Easterling
5	7223	E. V. Thomas
1	8524	J. A. Wackerly
5	3141	S. A. Landenberger
8	3141-1	C. L. Ward For DOE/OSTI
3	3151	W. I. Klein